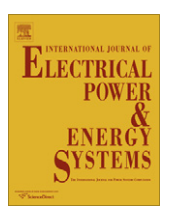
ELSEVIER

Contents lists available at SciVerse ScienceDirect

Electrical Power and Energy Systems

journal homepage: www.elsevier.com/locate/ijepes



A combined impedance and traveling wave based fault location method for multi-terminal transmission lines

E.E. Ngu*, K. Ramar

Faculty of Engineering, Multimedia University Malaysia, 63100 Cyberjaya, Malaysia

ARTICLE INFO

Article history:
Received 20 September 2010
Received in revised form 10 May 2011
Accepted 13 August 2011
Available online 7 October 2011

Keywords: Fault location Impedance based Multi-terminal line Traveling wave based

ABSTRACT

A new fault location method suitable for multi-terminal transmission lines that combines the advantages of both impedance and traveling wave based methods has been developed and presented in this paper. The proposed method first determines whether the fault is grounded or ungrounded by comparing the magnitude of the ground mode wavelet coefficients at the measurement end. Next, the impedance based method is used to identify the faulted half of the line in the case of two-terminal line and the faulted line section as well as the faulted half of the line section in the case of multi-terminal lines. Finally the fault location is determined by taking the time difference between the first two consecutive aerial modes of the current traveling waves observed at one end of the multi-terminal line. The proposed method has been tested on four- and five-terminal transmission lines with different types of faults, fault resistances and fault inception angles using ATP simulation.

© 2011 Elsevier Ltd. All rights reserved.

1. Introduction

Location of faults in power transmission lines is one of the main concerns for all the electric utilities as the accurate fault location can help to restore the power supply in the shortest possible time. Fault location methods for transmission lines are broadly classified as impedance based method which uses the steady state fundamental components of voltage and current values [1-3], traveling wave (TW) based method which uses incident and reflected TWs observed at the measuring end(s) of the line [4,5], and knowledge based method which uses artificial neural network and/or pattern recognition techniques [6,7]. All the above methods use the measured data either from one end of the transmission line or from all ends. The method which uses the data from all ends requires synchronized measurement with time stamping and online communication of data to one central location [8-13]. On the other hand, the one-end method which does not require synchronous measurement and online communication of data is simpler to apply to multi-terminal lines.

The one-end fault location method applicable to all types of faults using TWs requires identification of the faulted half of the line in the case of two-terminal line [14], and the faulted line section as well as the faulted half of the line section in the case of multi-terminal lines. A method of identifying the faulted half of the line in the case of two-terminal line using the polarities of wavelet transform coefficients (WTCs) is reported in [10]. Another method

of identifying the faulted line section and the faulted half of the line section for three-terminal line using the peak value of WTC is presented in [7]. These methods are found to be unreliable for multi-terminal lines. A method which combines the impedance based method with the TW based method to locate the fault in two-terminal line is reported in [15–17]. Here, the impedance based method is used first to find the fault location approximately and the accuracy is then improved by TW based method. As the fault location is determined approximately in this case using the impedance based method there is no need to identify the faulted half of the line. A method using the cross correlation between the forward and backward TWs to identify the fault location is proposed in [18]. It may be noted that the methods reported in [15–18] are applicable to two terminal lines only.

In this paper a fault location technique applicable to multi-terminal lines is presented. It is the extension and generalization of the method reported in [14] for two-terminal line. The developed method combines the simplicity of the impedance based method with the accuracy of the TW based method. A simplified impedance based method is used to identify the faulted line section and the faulted half of the line section. Daubechies-4 (db-4) mother wavelet is chosen for the Discrete Wavelet Transform (DWT) analysis of the current signal to obtain the time information of the incident and reflected TWs. The accurate fault location is then determined using these time information. The proposed algorithm is tested by simulating four- and five-terminal lines under different fault conditions such as various fault inception angles, fault distances and fault resistances. The constant distributed parameter line model (Clarke model) is used for simulation.

^{*} Corresponding author.

E-mail addresses: eengu@mmu.edu.my (E.E. Ngu), ramar@mmu.edu.my (K. Ramar).

The fundamental principle of the proposed fault location algorithm for multi-terminal lines is explained in Section 2. Test systems considered to explain the proposed method is discussed in Section 3. The test results and discussion on the results are presented in Section 4 and the conclusion is given in Section 5.

2. Fault location method for N-terminal lines

The fault location algorithm applicable to N -terminal lines (N > 2) presented in this paper is the combination of impedance and TW based methods.

The algorithm involves three major steps: (i) determination of the fault type (grounded or ungrounded), (ii) identification of the faulted line section and the faulted half of the line section in the case of grounded fault, and (iii) computation of fault distance using the incident and reflected (aerial mode) current traveling wave (CTW) at the measuring end. This has been summarized in the flow chart given in Fig. 1. It is assumed that the measurements are done at all the ends of the line independently (not synchronously) and there is no online communication between the terminals. Therefore, this method can also be termed as a one-end method.

2.1. Determination of fault type

As the TW based method employed in this paper is dependent on the type of fault, it becomes essential to identify whether it is grounded or ungrounded. The fault type can be determined using the method proposed in [5] which is based on the ground mode level-1 detailed (D1₀), WTC. If the magnitude of D1₀, WTC is found to be insignificant then the fault is ungrounded. Otherwise, it is grounded. The fault type can also be easily determined using the zero-sequence current computed using the data available at the measuring ends of the line. The presence of zero-sequence current indicates the fault is grounded, otherwise it is ungrounded. The

three-phase symmetrical fault is considered as an ungrounded fault.

2.2. Principle of TW based fault location

2.2.1. Discrete Wavelet Transform (DWT)

Before explaining the TW based fault location method a brief discussion of the Wavelet Transform (WT) and how to extract the WT coefficients are presented here. Wavelet-based technique has the ability to extract low- or high-frequency information from the signals of the power network that contains local discontinuities and/or disturbances by properly choosing the window size [19]. DWT is the discrete version of the Wavelet analysis and is defined by the equation

$$W(j,k) = \sum_{j} \sum_{k} x(k) 2^{-j/2} \varphi(2^{-j}n - k)$$
 (1)

where $\varphi(k)$ is the mother wavelet. DWT is a kind of multiresolution analysis, where the signal is analyzed at different frequencies with different resolutions. The analyzed signal is then decomposed into approximation and detail coefficients. The approximation coefficients are further decomposed into another set of approximation and detail coefficients. The process is then repeated and the successive stages of decomposition are known as level-1, level-2, etc. The detail coefficient of level 1 (D1) contains the high frequency information of the signal. The choice of mother wavelet plays a significant role in the analysis and db-4 mother wavelet has been adopted in this paper. The WTCs are obtained using MATLAB WT toolbox.

2.2.2. TW base fault location

Figs. 2 and 3 show the Lattice diagrams of aerial-mode TWs for ungrounded and grounded faults in the first half and the second half of a two-terminal transmission line, respectively. From the figures it can be observed that for the case of ungrounded fault the

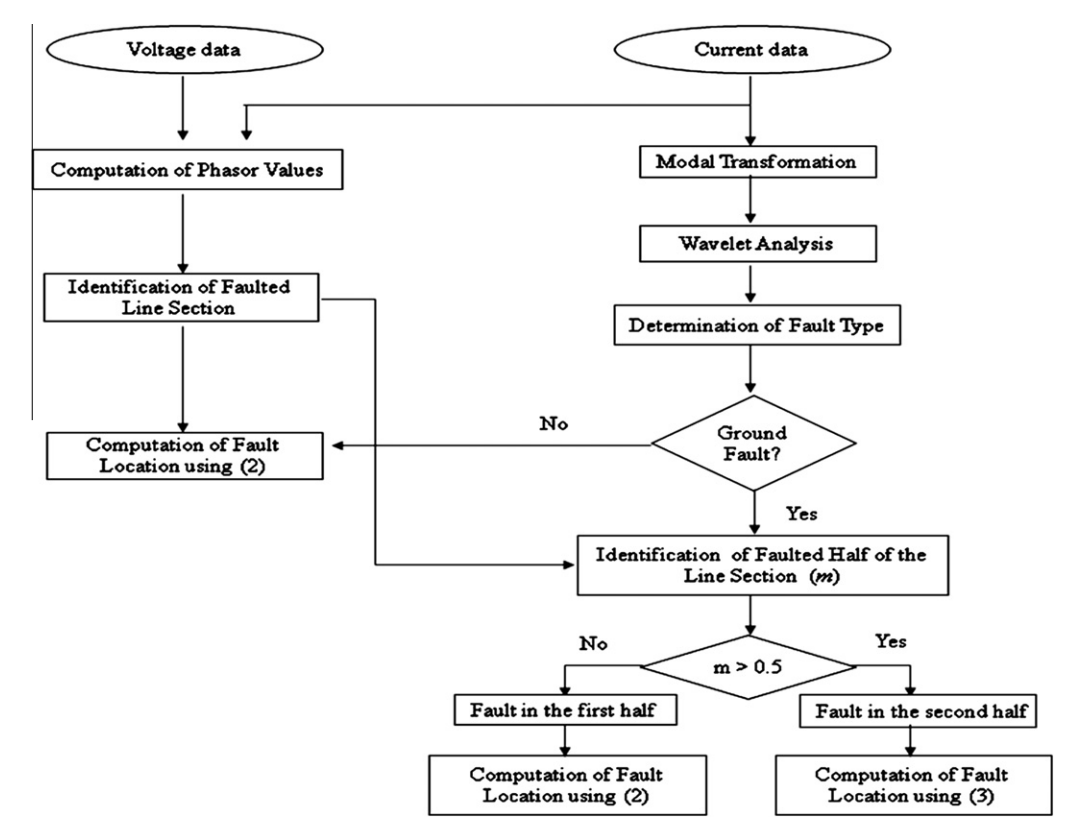


Fig. 1. Flowchart of the proposed fault location algorithm.

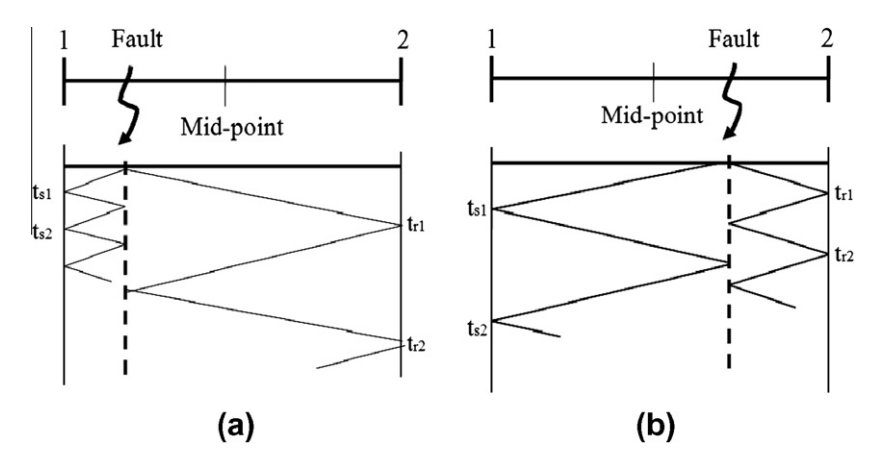


Fig. 2. Ungrounded fault in (a) first half and (b) second half of the line.

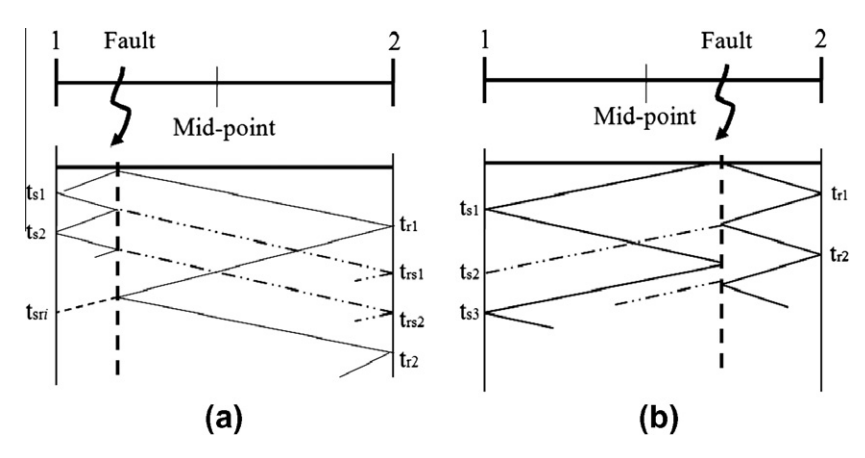


Fig. 3. Grounded fault in (a) first half and (b) second half of the line.

wave reflected from the remote terminal is not observed in the measuring terminal. This is because the transmission/refraction coefficient at the fault is negligibly small for the wave reflected from the remote end [11]. Hence the fault distance (x) for ungrounded faults (either in the first half or in the second half of the line) can be calculated using (2).

$$x = (t_{s2} - t_{s1})v/2 (2)$$

where $t_{s2} - t_{s1}$ is the time difference between the first two consecutive aerial mode TWs measured at terminal-1 (T-1) and ν is the aerial mode wave propagation velocity, which may be taken as 2.93953×10^5 km/s. For the grounded fault the wave reflected from the remote terminal will be observed at the measuring terminal. Therefore, (2) is used for the faults in the first half of the line. Whereas for the ground fault in the second half of the line, the fault distance is computed using

$$x = L - [(t_{s2} - t_{s1})v/2]$$
 (3)

where *L* is the length of the line. In case the fault is exactly at the midpoint of the line it may be considered as the fault in the first half of the line.

2.3. Identification of the faulted line section and faulted half of the line section

From the discussion in Section 2.2.2 it is clear that, for grounded faults, the identification of the faulted half of the line section is essential for accurate fault location using TW based method. The impedance based method is employed to identify the faulted line

section and the faulted half of the line section. This is explained first for two-terminal line and then for N-terminal line, where $N \ge 3$.

2.3.1. Two-terminal line

It is obvious that for two-terminal line, identification of the faulted half of the line only is required. For this purpose the impedance based method presented in [20] is applied after simplification. It is assumed that the phase angle difference between the fault current and the change in current at the sending end due to the fault is negligibly small. It is a valid assumption as this phase angle difference is normally very small. When the system is subjected to fault, the fundamental phasor quantities of during-fault current and during-fault voltage at the substation node 0 can be computed from the measured digital data by first removing the DC offset and then performing Digital Fourier analysis [21]. For this purpose the first cycle and one more sample of the fault data are used. During-fault currents and during-fault voltages will hereafter be called fault

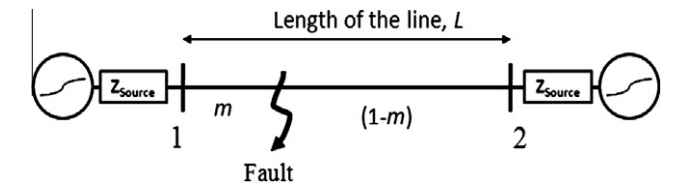


Fig. 4. Two-terminal equivalent power network with the fault at the fraction of the line length, m.

currents and fault voltages. The simplified algorithm presented here does not require any iteration. Consider a two-terminal transmission line shown in Fig. 4.

It is assumed the fault is at a distance mL from T-1 where m is the fault distance in the fraction of the line length. m can be computed for the ground fault in phase 'A' (A–G) and phase-to-phase-to-ground fault involving phases 'B' and 'C' (B–C–G) using (4) and (5), respectively [20]

$$m = imag\{V_{1a}(\Delta I_{1a} - \Delta I_{1a}^{o})^{*}\}/imag\{Z_{1}I_{1}(\Delta I_{1a} - \Delta I_{1a}^{o})^{*}\}$$
(4)

$$m = imag\{V_{1b} - V_{1c}\}/imag\{(Z_2 - Z_3)I_1\}$$
 (5)

where V_{1a} , V_{1b} , and V_{1c} are the phasor values of the three-phase voltages at T-1 at fault condition, I_1 is the three-phase fault current vector at T-1, ΔI_{1a} is the difference between fault and pre-fault currents in phase-A (pure fault component of the current), ΔI_{1a}^o is the difference between the zero-sequence fault and pre-fault currents, Z_i denotes the ith row of the line impedance matrix (Z), imag{} denotes the imaginary part of the complex number within the brackets and the superscript * refers to the complex conjugate.

For three-phase and phase-to-phase (B-C) faults, m is computed using (6) and (7), respectively.

$$m = imag\{V_{1a}\Delta I_{1a}^*\}/imag\{ZI_{1a}\Delta I_{1a}^*\}$$
(6)

$$m = imag\{(V_{1b} - V_{1c})\Delta I_{1b}^*\}/imag\{(Z_2 - Z_3)I_1.\Delta I_{1b}^*\}$$
 (7)

In the above equations, Z is the positive sequence impedance of the line; ΔI_{1b} is the difference between the fault current and the pre-fault current in phase-B. Other symbols have been defined earlier. Once the value of m is computed the faulted half of the line is identified as:

- (i) The first half of the faulted line if $0 < m \le 0.5$.
- (ii) The second half of the faulted line if 0.5 < m < 1.0.

2.3.2. N-terminal line $(N \ge 3)$

The procedure of identifying the faulted line section and the faulted half of the line section is explained here by considering a five-terminal line shown in Fig. 5.

In the case of five-terminal line m is first computed for the line section 1-3 using the voltage and current available at T-1. Depending on the type of fault any one of the above four Eqs. (4)–(7) is used. If calculated m < 1, then the line section 1-3 is the faulted line section. If not, the procedure of computing m is continued using the data available at terminal 2 (T-2). If m < 1, then line section 2-3 is the faulted line section. Continuing this procedure, the faulted line section is identified if the fault is in any one of the 'outer' line sections 1-3, 2-3, 4-5, 6-7, and 8-7. If all the values of m > 1 then the fault is in one of the 'inner' line sections 3-5 and 5-7. To identify the faulted line section between these two, we have to compute the voltage and current values at junction

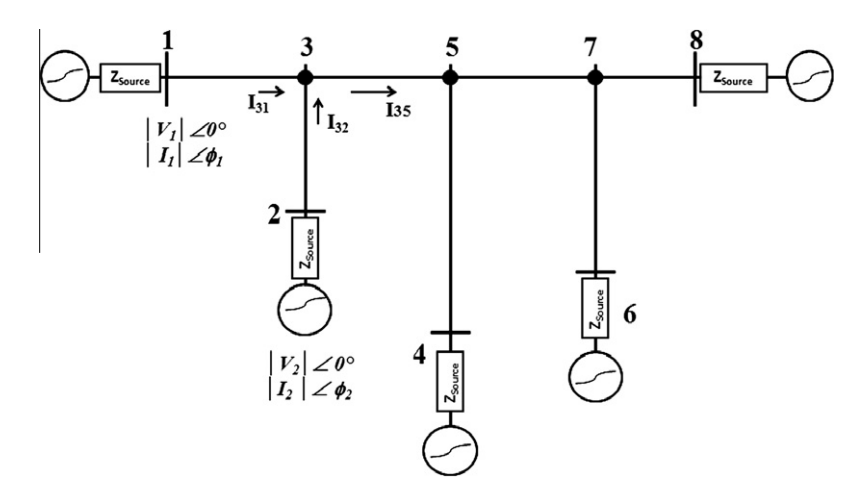


Fig. 5. Equivalent circuit of a five-terminal transmission line with the fault voltages and currents marked at terminals 1 and 2.

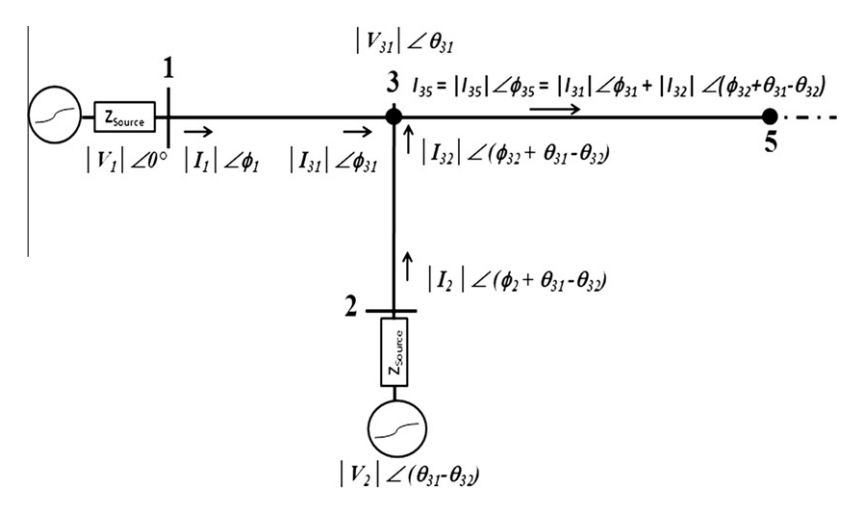


Fig. 6. Voltage and current at J-3.

3 (J-3) or junction 7 (J-7). From the measured values of voltages and currents at T-1 and T-2, the voltage at J-3 and the current flowing from J-3 toJ-4 can be computed. It is worth noting that as there are no synchronous measurements, the phasor values of voltages and currents computed at the outer terminals are not with respect to a common base.

Let $V_1 = |V_1| \angle 0^\circ$, $I_1 = |I_1| \angle \phi_1$ and $V_2 = |V_2| \angle 0^\circ$, $I_2 = |I_2| \angle \phi_2$ be the fault voltage and current at T-1 and T-2, respectively. Let the voltage at J-3 and the current entering J-3 from T-1 be $V_{31} \angle \theta_{31}$, $I_{31} \angle \phi_{31}$, respectively. Then we can write

$$\begin{bmatrix} |V_{31}| \angle \theta_{31} \\ |I_{31}| \angle \phi_{31} \end{bmatrix} = \begin{bmatrix} A & -B \\ -C & D \end{bmatrix} \begin{bmatrix} |V_1| \angle 0 \\ |I_1| \angle \phi_1 \end{bmatrix}$$
(8)

where *A*, *B*, *C*, *D* parameters are for the line section 1-3. In a similar manner we can compute the fault voltage at J-3, $|V_{32}| \angle \theta_{32}$ and the fault current entering J-3 from T-2, $|I_{32}| \angle \phi_{32}$ using the voltage and current at T-2. As there is no fault in sections 1-3 and 2-3 the magnitude of the voltages V_{31} and V_{32} will be identical, but the phase angle θ_{31} may not be equal to θ_{32} due to unsynchronized measurement at the terminals. Taking the measurement at T-1 as the reference, the phase angle of voltage at T-2 can be corrected to yield the same phase angle for V_{31} and V_{32} . The corrected values are: $|V_1|\angle 0^\circ$, $|I_1|\angle \phi_1$, $|V_2|\angle (\theta_{31}-\theta_{32})$, $|I_2|\angle (\phi_2+\theta_{31}-\theta_{32})$, $|V_{31}|\angle \theta_{31}$, $|I_{31}|\angle \phi_{31}$, and $|I_{32}|\angle (\phi_{32}+\theta_{31}-\theta_{32})$. Therefore the fault current flowing from J-3 to J-5 is $|I_{35}|\angle \phi_{35}=|I_{31}|\angle \phi_{31}+|I_{32}|\angle (\phi_{32}+\theta_{31}-\theta_{32})$.

Fig. 6 shows these voltage and current values. Similarly, the prefault voltage and current at J-3 are calculated. Using these values, m for the line section 3-5 is calculated using any one of the four Eqs. (4)–(7). If m is less than 1 then the fault is in line section 3-5. The faulted half of the line section is also identified, if required, using the same m value. If m is greater than 1 then the procedure is continued by computing the voltage current values at J-5. The next step in the fault location algorithm is the computation of fault distance using incident and reflected TWs at the outer terminals.

2.4. Computation of fault distance

Once the faulted line section and faulted half of the line section are known the accurate fault distance is computed using the TW based method explained in Section 2.2.2. For this purpose the time of arrival of the incident and reflected TWs at the terminal nearest to the fault (based on the value of m determined from the impedance based method) is determined by performing DWT on the current signal measured at that terminal. As a matter of fact the fault distance may be computed by observing the time of arrival of the incident and reflected TWs at T-1 for all the type of faults. But, here we recommend to use the measurements at the terminal nearest to the fault because the strength of the TWs at the nearest terminal will be stronger compared to that observed in other terminals.

For example consider an L–G fault (ground fault) in the second half of the line section 3-5 (Refer to Fig. 5). The nearest terminal is determined based on the m value and the actual length of each line section. For this fault let T–2 be the nearest terminal. Observing $t_{\rm s1}$ and $t_{\rm s2}$, the location of the fault is computed to be at a distance of

$$x = L_{35} - [(t_{s2} - t_{s1})\nu/2]$$
 (9)

from J-3. Similarly for an L-L fault (ungrounded fault) in the second half of the line section 3-5 the fault distance from J-3 is

$$x = (t_{s2} - t_{s1})v/2 \tag{10}$$

In a similar way the fault distance for any type of fault at any line section can be computed. The time information (t_{s1} and t_{s2}) from the measured current signals at the terminals is extracted using the first level of the detailed WTCs.

3. Test System

To explain the procedure discussed in Section 2, two 400-kV Power Transmission Systems one with four terminals and the other with five terminals are considered. The tower configuration [22] of the transmission lines in both the system is the same and is given in Fig. 7.

The four- and the five-terminal power transmission lines with their Thevenin's equivalent source impedances at all ends of the line are shown in Fig 8. The Thevenin's equivalent source impedances at all ends of the line are modeled using symmetric RL coupled lines [23] and the values of the positive and zero sequence equivalent source resistances and inductances are $R_1 = 0.06 \Omega$, $R_0 = 0.13 \Omega$, $L_1 = 39.99 \text{ mH}$ and $L_0 = 23.71 \text{ mH}$.

For simplicity it is assumed that the phase angle difference between voltages of the source generators to be zero. As suggested in [4], busbars at each end of the line should be modeled by capacitors connected to the ground as the busbars of the line will be dominated by the capacitors during high frequency transient event and hence a capacitance of 0.001 µF has been chosen in this work.

The length of each line section is given in the figure. The required data for this line model such as positive- and zero-sequence line impedances in Ω per unit length (Ω/km), surge impedance in Ω and TW propagation velocity in length per second are calculated using Line Constants supporting program [24] available in ATP. The input data information for the program are: the size and resistance per unit length of conductors and shield wires, separation between the phase conductors, height of the conductors and shield wires above the ground level, etc. For more detailed information on input parameters for each conductor and shield wire [22] may be referred to.

The 50-Hz, 400-kV multi-terminal line is modeled using transposed distributed parameter (Clarke) model and simulated using ATPDraw™, a graphical and mouse-driven pre-processor to the ATP version of the Electromagnetic Transients Program (EMTP) [25]. A perfect conducting ground condition is assumed. The output of the simulation is converted into .MAT file for phasor computation and DWT analysis in MATLAB. The fault is created at different locations under various conditions, such as different fault resistances, fault inception angles and fault types and the results are discussed in the next section. A sampling frequency of 1 MHz has been used in the simulation.

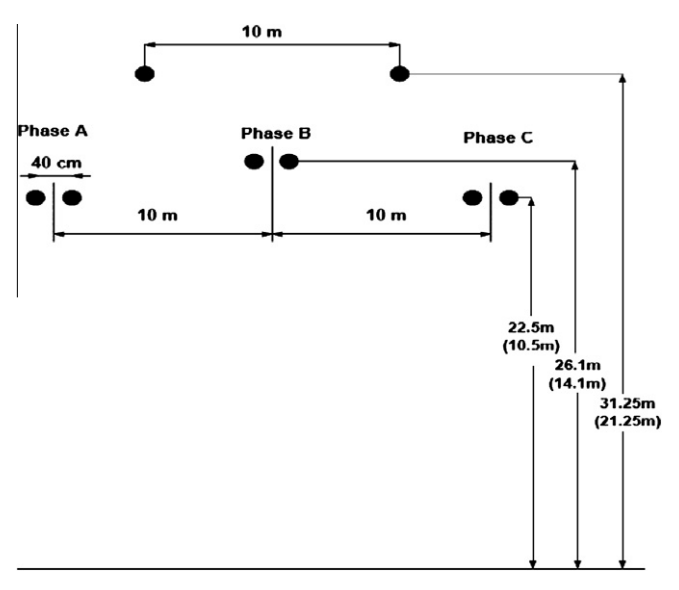


Fig. 7. Tower configuration of the 400-kV test systems.

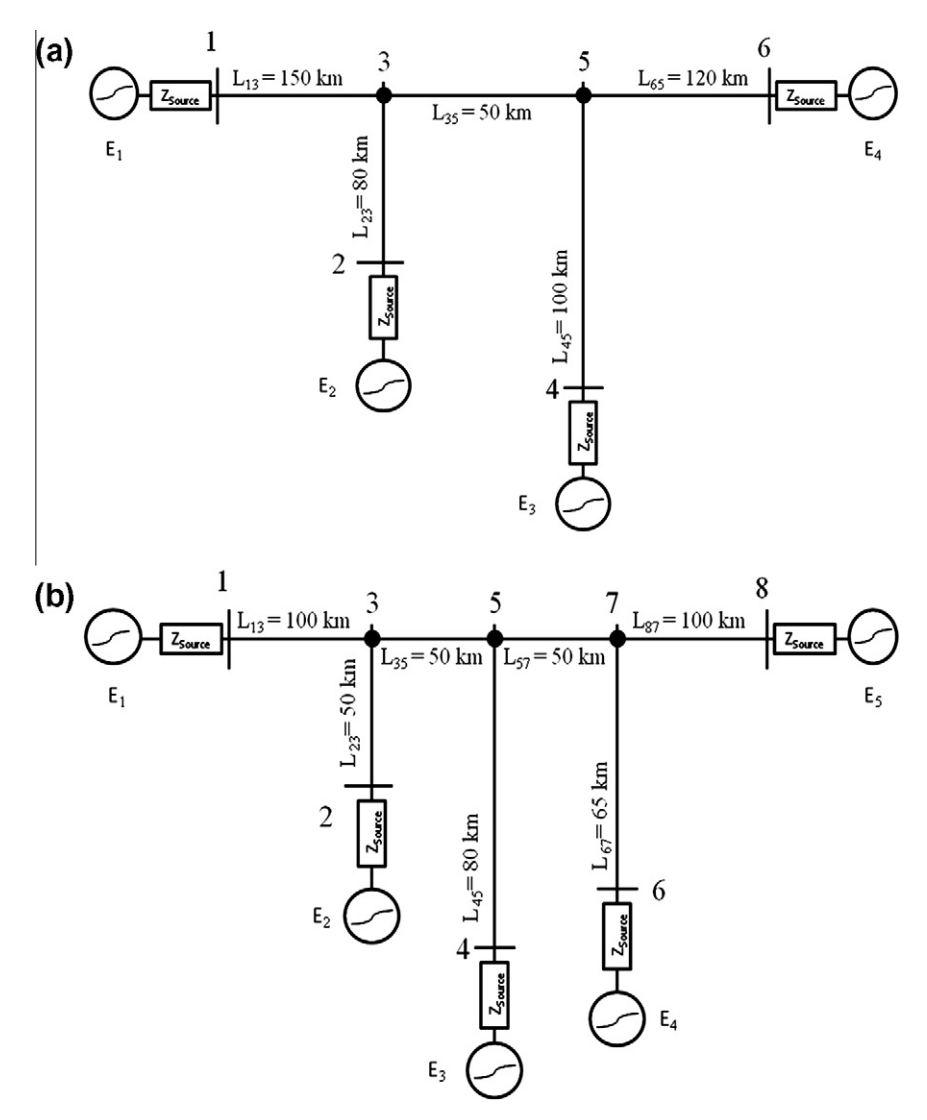


Fig. 8. A 400-kV (a) four-terminal and (b) five-terminal power transmission lines with their Thevenin's equivalent source impedances at all terminals.

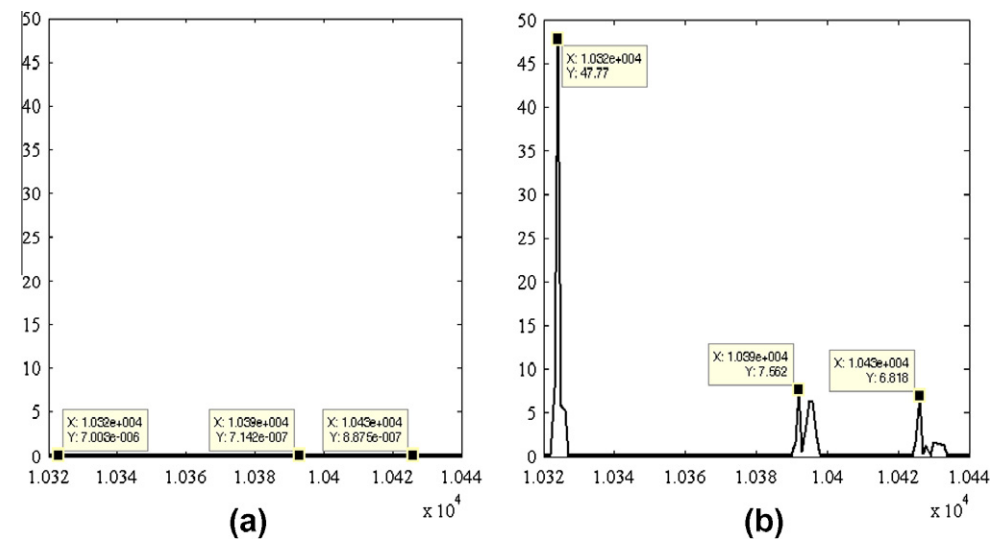


Fig. 9. The magnitude of D1₀, WTC at T-1 for (a) B-C (ungrounded) and (b) A-G (grounded) faults occurred at 30 km from J-3 of the four-terminal line.

Table 1Fault location results of the various types of faults on the four-terminal power transmission line.

Faulted line segment	Fault created at x km	Fault type	Fault resistance (Ω)	Calculate junction		e using da	ta at term	inal/	Results of i method	mpedance based	x calculated by TW (km) from terminal/junction	Error (%)
				T-1	T-2	T-4	T-6	J-3	Faulted line segment	Faulted half		
1-3		A-G	0	0.8267	_	_	_	_	1-3	2nd half	120.0168 (T-1)	0.0112
			25	0.8213	-	-	-	-	1-3	2nd half	120.0168 (T-1)	0.0112
			50	0.8236	-	-	-	-	1-3	2nd half	120.0168 (T-1)	0.0112
	120 from T-1	B-C-G	0	0.8317	-	_	_	_	1-3	2nd half	120.0168 (T-1)	0.0112
			25	0.8287	-	-	-	-	1–3	2nd half	120.0168 (T-1)	0.0112
			50	0.8302	-	-	-	-	1–3	2nd half	120.0168 (T-1)	0.0112
		B-C	N/A	0.8252	-	-	-	-	1-3	2nd half	119.9328 (T-1)	0.0448
2–3		A-G	0	2.2029	0.1925	_	_	_	2-3	1st half	14.9916 (T-2)	0.0105
			25	1.9433	0.2066	-	-	-	2-3	1st half	14.9916 (T-2)	0.0105
	15 from T-2		50	1.7260	0.2224	-	-	-	2-3	lst half	14.9916 (T-2)	0.0105
		B-C-G	0	2.2394	0.1940				2-3	lst half	14.9916 (T-2)	0.0105
			25	2.2374	0.1934	-	-	-	2-3	1st half	14.9916 (T-2)	0.0105
			50	2.2380	0.1938	-	-	-	2-3	lst half	14.9916 (T-2)	0.0105
		B-C	N/A	2.2165	0.1938				2-3	_	14.9916 (T-2)	0.0105
4-5		A-G	0	3.3564	3.5899	0.6133	_	_	4-5	2nd half	60.0224 (T-4)	0.0224
			25	3.1664	3.4765	0.6230	_	_	4-5	2nd half	60.0224 (T-4)	0.0224
	60 from T-4		50	3.0030	3.3762	0.6347	_	_	4-5	2nd half	60.0224 (T-4)	0.0224
		B-C-G	0	3.3585	3.6827	0.6213			4-5	2nd half	60.0224 (T-4)	0.0224
			25	3.3519	3.6737	0.6190	-	-	4-5	2nd half	60.0224 (T-4)	0.0224
			50	3.3552	3.6784	0.6203	-	-	4-5	2nd half	60.0224 (T-4)	0.0224
		B-C	N/A	3.3169	3.6487	0.6176	-	-	4-5		60.0336 (T-4)	0.0336
5-6		A-G	0	5.0897	5.4645	2.8220	0.3404	_	5-6	2nd half	39.9776 (T-6)	0.0187
			25	4.5904	5.0807	2.6777	0.3484	_	5-6	2nd half	39.9776 (T-6)	0.0187
	40 from T-6		50	4.1748	4.7661	2.5639	0.3574	-	5-6	2nd half	39.9776 (T-6)	0.0187
		B-C-G	0	5.0134	5.5222	2.8726	0.3450		5-6	2nd half	39.9776 (T-6)	0.0187
			25	5.0056	5.5114	2.8664	0.3437	-	5-6	2nd half	39.9776 (T-6)	0.0187
			50	5.0086	5.5164	2.8694	0.3444	-	5-6	2nd half	39.9776 (T-6)	0.0187
		B-C	N/A	4.9416	5.4640	2.8469	0.3434	-	5-6	-	39.9776 (T-6)	0.0187
3–5		A-G	0	1.5896	1.6511	1.4244	1.4107	0.6310	3-5	2nd half	30.0111 (J-3)	0.0224
			25	1.5537	1.6432	1.4052	1.3835	0.6222	3-5	2nd half	30.0111 (J-3)	0.0224
	30 from J-3		50	1.5219	1.6434	1.4017	1.3740	0.6165	3-5	2nd half	30.0111 (J-3)	0.0224
	-	B-C-G	0	1.5977	1.6780	1.4321	1.4173	0.6544	3-5	2nd half	30.0111 (J-3)	0.0224
			25	1.5935	1.6728	1.4277	1.4133	0.6496	3-5	2nd half	30.0111 (J-3)	0.0224
			50	1.5957	1.6756	1.4300	1.4154	0.6521	3-5	2nd half	30.0111 (J-3)	0.0224
		B-C	N/A	1.5815	1.6651	1.4204	1.4050	0.6396	3-5	_	29.9832 (J-3)	0.0336

Using very high sampling frequency of 1 MHz does not impose any stringent requirements on CTs and the data acquisition systems as high sampling frequency recorder (100 kHz-4 MHz) and high bandwidth CTs are commercially available [26,27].

4. Results and discussions

4.1. Fault type determination

As explained in Section 2.1 the fault type is determined based on D1₀, WTC. For example consider grounded (A–G) and ungrounded (B–C) faults on the line section 3-5 of the five-terminal transmission line at a distance of 30 km from J-3. Fig. 9a and b shows the magnitude of D1₀, WTC of the incident TW at T-1 for B–C and A–G faults, respectively. It is observed clearly that the peak of the WTC of the incident wave at T-1 for the grounded fault is very significant compared to the ungrounded fault. Hence the fault type can be determined using D1₀, WTC. This procedure can be employed to identify the fault type for the all cases reported in this section.

4.2. Fault location

The proposed fault location algorithm has been tested for the four- and five-terminal lines with different types of faults. More

than 100 cases for each type of line have been tested. But, for want of space, only a few cases are reported in this section. Table 1 and Table 2 show the results for four- and five-terminal transmission line systems, respectively.

4.2.1. Four-terminal transmission line

For example consider an A–G fault in the line section 3-5 of the four-terminal line with a fault resistance of 25 Ω at a distance of 30 km from J-3. Using the phasor measurements at T-1, T-2, T-4 and T-6 the value of m is computed to be more than 1. This indicates that the fault is not in the outer line sections 1-3, 2-3, 4-5, and 6-5. By computing the voltage and current phasors at J-3, m is calculated to be 0.6222 which indicates that the fault is in the second half of the faulted line section 3-5. Fig. 10 shows the incident and reflected detail level-1 WTC observed at T-2. From t_{s1} and t_{s2} the fault distance is computed using (9) as 30.0112 km from J-3.

The error in fault location is 0.0112 km and the corresponding percentage error based on the length of the line section 3-5 is 0.0224%. In a similar way the fault location is determined for other types of faults and tabulated.

For faults that are very near to the line junctions or the mid point of the line sections the impedance based algorithm may identify the faulted line section and the faulted half of the line section wrongly. Therefore the fault location computed using the TWs based on the line section identified by the impedance based

Table 2Results of the various tests conducted on the five-terminal power transmission lines for A–G, B–C–G and B–C faults.

Faulted line section	Fault distance (km)	Fault	Fault resistance (Ω)	Calculate	d m value	at each te	rminal/ju	Identified by impedance based method		<i>x</i> calculated by TW based	Error (%)			
				T-1	T-2	T-4	T-6	T-8	J-3	J-5	Line section	Fault half	(km) al terminal/ junction	
1–3	30 from T-1	A-G	0	0.304	_	_	_	_	_	_	1-3	lst half	29.9832 (T-1)	0.0168
			25	0.319	-	-	-	_	_	-	1-3	lst half	29.9847 (T-1)	0.0153
			50	0.333	-	-	-	_	_	-	1-3	1st half	29.9832 (T-1)	0.0168
		B-C-G	0	0.310	-	-	-	-	-	-	1-3	lst half	29.9832 (T-1)	0.0168
			25	0.309	-	-	-	-	-	-	1–3	lst half	29.9832 (T-1)	0.0168
			50	0.310	-	-	-	-	-	-	1–3	1st half	29.9847 (T-1)	0.0153
		B-C	0	0.309	-	-	-	-	-	-	1–3	-	29.9832 (T-1)	0.0168
2-3	20 from T-2	A-G	0	1.7334	0.4080	-	_	_	_	-	2-3	lst half	19.9888 (T-2)	0.0224
			25	1.6144	0.4430	-	-	_	_	-	2-3	lst half	19.9903 (T-2)	0.0194
			50	1.5131	0.4792	_	_	_	_	_	2-3	1st half	19.9888 (T-2)	0.0224
		B-C-G	0	1.7587	0.4132	-	-	-	_	-	2-3	lst half	19.9888 (T-2)	0.0224
			25	1.7570	0.4123	-	-	-	-	-	2-3	lst half	19.9888 (T-2)	0.0224
			50	1.7582	0.4131	-	-	_	_	-	2-3	1st half	19.9888 (T-2)	0.0224
		B-C	0	1.7508	0.4120						2-3		19.9888 (T-2)	0.0224
4–5	15 from T-4	A-G	0	6.0631	7.0366	0.1907	_	_	_	_	4-5	1st half	14.9916 (T-4)	0.0105
			25	5.2162	6.3397	0.2099	_	_	_	_	4-5	1st half	14.9916 (T-4)	0.0105
			50	4.4850	5.7253	0.2293					4-5	1st half	14.9916 (T-4)	0.0105
		В-С-С	0	5.9625	7.2311	0.1937					4-5	1st half	14.9816 (T-4)	0.0105
			25	5.9591	7.2268	0.1934					4-5	1st half	14.9916 (T-4)	0.0105
			50	5.9596	7.2297	0.1938					4-5	1st half	14.9916 (T-4)	0.0105
		B-C	0	5.9929	7.0663	0.1931					4-5	_	14.9916 (T-4)	0.0105
	45 from T C	۸ ،	0				0.7122					2-4 6-16		
6–7	45 from T-6	A–G	0 25	7.1979 6.4387	8.3774 7.7922	3.4002	0.7123	-	_	-	6-7	2nd half 2nd half	45.0112 (T-6)	0.0172
			50	5.8515	7.7922	3.2309 3.1091	0.7316 0.7577	_	_	_	6–7 6–7	2nd half	45.0112 (T-6) 45.0112 (T-6)	0.0172 0.0172
		B-C-G	0	6.8849	8.3830	3.5125	0.7377	_	_	-	6–7 6–7	2nd half	45.0112 (T-6)	0.0172
			25	6.8779	8.3719	3.5073	0.7133				6–7	2nd half	45.0112 (T-6)	0.0172
			50	6.8817	8.3797	3.5112	0.7143	_			6-7	2nd half	45.0112 (T-6)	0.0172
			0	7.0380	8.3082	3.3774	0.7110	_	_	_	6-7	- Liid iidii	44.9748 (T-6)	0.0172
8–7	60 from T-8	A-G B-C-G	0	10.0313	11.6169	4.7428	2.2408	0.6130		-	8-7	2nd half	60.0224 (T-4)	0.0224
			25	9.1001	10.9161	4.5268	2.2212	0.6245	-	-	8-7	2nd half	60.0239 (T-4)	0.0239
			50	8.2764	10.3085	4.3550	2.2101	0.6383			8-7	2nd half	60.0224 (T-4)	0.0224
			0	9.4171	11.5125	4.9005	2.3194	0.6195			8-7	2nd half	60.0224 (T-4)	0.0224
			25 50	9.4057 9.4110	11.4937 11.5049	4.8914 4.8972	1.8800 1.8830	0.6177 0.6189			8–7 8–7	2nd half	60.0224 (T-4)	0.0224
		В-С	0	9.4110	11.5049	4.8972	2.2972	0.6148			8-7 8-7	2nd half	60.0224 (T-4) 59.9664 (T-4)	0.0224 0.0336
													, ,	
3–5	5 from J-3	3 A-G	0	1.1647	1.1813	2.2202	4.8939	4.5374	0.1186	-	3–5	1st half	4.9972 (J-3)	0.0056
			25	1.1458	1.2177	2.1679	4.6584	4.2175	0.1145	-	3–5	1st half	4.9972 (J-3)	0.0056
			50	1.1358	1.2532	2.1262	4.4465	3.9300	0.1161		3–5	1st half	4.9972 (J-3)	0.0056
		B-C-C	0	1.1684	1.2030	2.1493	4.6795	4.1837	0.1247		3-5	1st half	4.9972 (J-3)	0.0056
			25	1.1665	1.2006	2.2866	4.9561	4.4222	0.1240		3-5	1st half	4.9972 (J-3)	0.0056
		D 6	50	1.1680	1.2026	2.2895	4.9611	4.4257	0.1252		3-5	1st half	4.9972 (J-3)	0.0056
		B-C	0	1.1565	1.1937	2.2481	4.8427	4.5193	0.1171		3–5	=	4.9972 (J-3)	0.0056
5-7	40 from J-5	A-G	0	4.6114	5.3020	2.1136	1.2931	1.2690	2.6206	0.8424	5-7	2nd half	39.9910 (J-5)	0.0018
			25	4.2901	5.1117	2.0817	1.3105	1.2605	2.5474	0.8125	5-7	2nd half	39.9910 (J-5)	0.0018
			50	4.0432	4.9830	2.0646	1.3319	1.2555	2.5136	0.8018	5-7	2nd half	39.9910 (J-5)	0.0018
			0	4.4550	5.3515	2.1783	1.3156	1.2771	2.5923	0.8494	5-7	2nd half	39.9910 (J-5)	0.0018
		B-C-G	25	4.4496	5.3428	2.1744	1.3128	1.2748	2.5883	0.8480	5-7	2nd half	39.9910 (J-5)	0.0018
			50	4.4535	5.3496	2.1775	1.3150	1.2766	2.5918	0.8500	5-7	2nd half	40.0056 (J-5)	0.0112
		B-C	0	4.4803	5.2983	2.1308	1.3011	1.2650	2.5809	0.8298	5-7	_	39.9976 (J-5)	0.0048

algorithm may have large errors. A maximum error of 3 km for a grounded fault near the mid point of the outer line sections and 3.7 km for a fault near to the junction has been found.

4.2.2. Five-terminal transmission line

A few test results for this example system are given in Table 2. For example consider an A–G fault in line section 5-7 at a distance of 40 km from J-5. The fault resistance is $50\,\Omega$. For this case m computed by the impedance based algorithm using the phasor measurements at each line terminal is more than 1. Hence the fault is not in the outer line sections. Then the voltage and current phasors at J-3 have been computed to calculate the corresponding m. As this value of m is also found to be greater than 1, the voltage

and current phasors at J-5 have been computed as explained in Section 2.3.2. From this m value the fault is identified to be in the second half of the faulted line section 5-7.

Fig. 11 shows the time of arrival of the incident and the reflected TWs at T-6. From these timings the fault distance is calculated and the value is given in the table. Similar to four-terminal case here also it is observed that the error in fault location is very small when the faulted line and the faulted half of the line section are correctly identified. For faults near to the line junctions or the mid points of the line sections the error in fault location is found to be high. The maximum error has been found to be 4.5 km for a fault near to the junction J-3. The error can be reduced if a more accurate impedance based method is used.

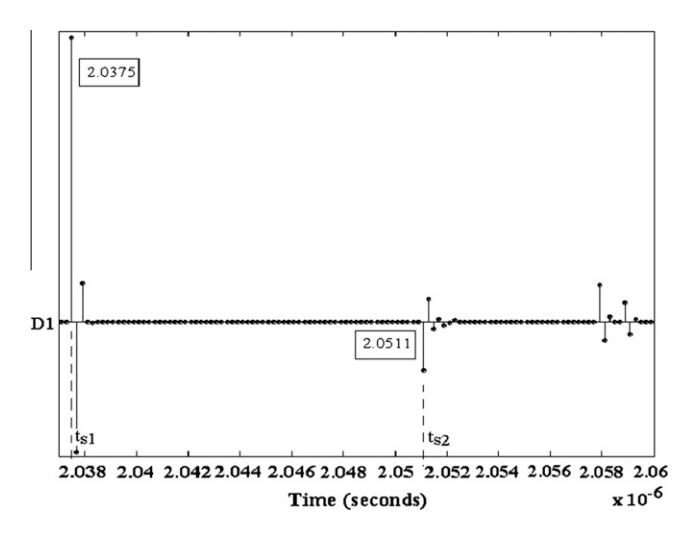


Fig. 10. Level 1 WTC observed at T-2 for A-G fault at 30 km from J-3, with fault resistance of 50 Ω .

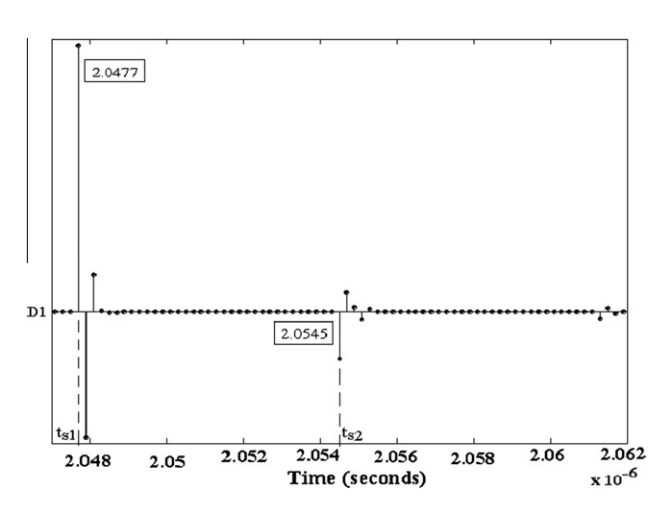


Fig. 11. Time of arrival of the incident and the reflected TWs at T-6, with fault resistance of 50 $\Omega.\,$

5. Conclusion

A fault location method, which combines the impedance based method and the TW based method to locate the fault accurately for multi-terminal transmission lines is proposed in this paper. Even though many impedance based methods and TW based methods are reported in the literature, suggestion of a simple and reliable impedance based method along with the accurate TW based algorithm and application of the method to multi-terminal lines are the novelty of this method. This method is an extension of the method reported in [14] for two-terminal lines. The efficacy of the proposed fault location method has been demonstrated by simulating two example systems under different fault conditions. The faults are simulated with different fault resistances, fault occurrence times, fault types, fault location and fault inception angles. Simulation results show that the proposed algorithm works satisfactorily for all types of faults. It has been found that once the faulted line section and the faulted half of the line section are identified correctly, regardless of the fault type, the fault location is computed with high accuracy. The error in the impedance based method in identifying the faulted line (for faults very near to the junction) and the faulted half of the line section (for faults very near to the mid points of the line sections) are mainly due to the extraction of the phasor values from the measured transient signals and the simplifying assumptions made in modeling the transmission lines. However the accuracy can be further improved for the above cases also if accurate impedance based method is employed.

References

- [1] Filomena AD, Resener M, Salim RH, Bretas AS. Extended impedance-based fault location formulation for unbalanced underground distribution systems. In: IEEE PESGM-conversion & delivery of electrical energy in the 21st century; 2008 July. p. 1–8.
- [2] Amir AA, Ramar K. Accurate one-end fault location for overhead transmission lines in interconnected power systems. Int J Electr Power Energy Syst 2010;32(5):383-9.
- [3] Abdel-Fattah M, Lehtonen M. A new transient impedance-based algorithm for earth fault detection in medium voltage networks. In: International conference on power systems transients, Kyoto, Japan; June 2009.
- [4] Bo ZQ, Johns AT, Aggarwal, AK. A novel fault locator based on the detection of fault generated high frequency transients. In: Proceedings of 6th IEE developments in power systems protection conference; March 1997. p. 197-200
- [5] Evrenosoglu CY, Abur A. Travelling wave based fault location for teed circuits. IEEE Trans Power Deliv 2005;20(2):1115–21.
- [6] Anamika Jain, Kale VS, Thoke AS. Application of artificial neural networks to transmission line faulty phase selection and fault distance location. In: IASTED, Chiang Mai, Thailand; 29–31 March 2006. p. 262–7.
- [7] Fernandez RMC, Rojas HND. An overview of wavelet transforms applications in power systems. In: 14th PSCC, Sevilla, Spain; 2002. p. 1–8.
- [8] Lee H. Development of accurate traveling wave fault locator using global positioning satellites. In: 20th Annual western protective relay conference, Spokane Washington, USA; October 1993. p. 197–204.
- [9] Jiang F, Bo ZQ, Weller G, Chin SM, Redfern MA. A GPS based fault location scheme for distribution line using wavelet transform technique. In: international conference on power system transients, Budapest, Hungary, June 1999, p. 224–8.
- [10] Elhaffar A, Lehtonen M. An improved GPS current traveling-wave fault locator in EHV transmission networks using few recordings. In: Proceedings of international conference on future power systems, Schiphol-Amsterdam, Netherlands; 1–5 November 2005.
- [11] Silva MD, Oleskovicz M, Coury DV. Hybrid fault locator for three-terminal lines based on wavelet transforms. Electr Power Syst Res 2008;78(11):1980-8.
- [12] Lin YH, Liu CW, Yu CS. A new fault locator for three-terminal transmission lines—using two-terminal synchronized voltage, current phasors. IEEE Trans Power Deliv 2002;17(2):452–9.
- [13] Chen CS, Liu CW, Fast and accurate fault detection/location algorithms for double-circuit/three-terminal lines using phasor measurement units. J Chin Inst Eng 2003;26(3):289–99.
- [14] Ngu EE, Ramar K. Single-ended traveling wave based fault location on two terminal transmission lines. In: IEEE TENCON, Singapore; 23rd-26th November, 2009. p. 1-4. ISBN: 978-1-4244-4547-9.
- [15] Zheng XY, Li XM, Ding JY, Duan ZY. Study on impedance-traveling wave assembled algorithm in one-terminal fault location system for transmission lines. In: 3rd International conference on electric utility deregulation & restructuring and power technologies; April 2008. p. 1123–6.
- [16] Yerekar SR. Fault location system for transmission lines in one-terminal by using impedance-traveling wave assemble. http://eeeic.eu/proc/technical_program_cd.html [accessed August 2009].
- [17] Dong XZ, Chen Z, He XZ, Wang KH, Luo CM. Optimizing solution of fault location. IEEE Power Eng Soc Summer Meet 2002;3:1113–7.
- [18] Rajendra S, McLaren PG. Traveling wave techniques applied to the protection of teed circuits: multi-phase/multi-circuit system. IEEE Trans Power Apparat Syst 1985 Dec:104:3351-7.
- [19] Vahidi B, Ghaffarzadeh N, Hosseinian SH. A wavelet-based method to discriminate internal faults from inrush currents using correlation coefficient. Int J Electr Power Energy Syst 2010;32(7):788–93.
- [20] Ramar K, Eisa AA. New fault location algorithms for overhead transmission lines. Int J Power Energy Syst 2008;28(2):241–51.
- [21] Eisa AA, Ramar K. Removal of decaying DC offset in current signals for power system phasor estimation. In: 43rd International universities power engineering conference; 2008. p. 1–4.
- [22] Martinez-Velasco JA. Computer analysis of voltage variations in power systems: lightning studies of transmission lines using the ATP/EMTP. http://www.ieeeprc.org/Activities/PR2V7BN.pdf> [accessed April 2009].
- [23] Elkalashy NI, Darwish HA, Taalab AMI, Izzularab MA. An adaptive single pole autoreclosure based on zero sequence power. Electr Power Syst Res 2007;77(5–6):438–46.
- [24] Canadian/American EMTP User Group. Alternative transients program rule book. European EMTP-ATP Users Group e.V.; 1987–1998.
- [25] Prikler LH, Høidalen K. ATPDraw Version 3.5 for Windows (Preliminary Release No. 1.1). http://www.elkraft.ntnu.no/atpdraw/ATPDMan3r3.pdf [accessed September 2008].
- [26] ISA Srl: "TFS 2100 Traveling Wave Fault Locator System". http://www.isatest.com/pdf/products/TFS2100.pdf [accessed May 2011].
- [27] Coggins D, Thomas D, Hayes-Gill B, Yiqun Zhu, Pereira ET, Cabral S. initial experiences with a new FPGA based traveling wave fault recorder installed on a MV distribution network. POWERCON; 1–9 October, 2008.